

# Self-accelerating Massive Gravity: Superluminality, Cauchy Surfaces and Strong Coupling

Pavel Motloch,<sup>1</sup> Wayne Hu,<sup>2</sup> Austin Joyce,<sup>2</sup> and Hayato Motohashi<sup>2</sup>

<sup>1</sup>*Kavli Institute for Cosmological Physics, Department of Physics,  
University of Chicago, Chicago, Illinois 60637, U.S.A*

<sup>2</sup>*Kavli Institute for Cosmological Physics, Department of Astronomy & Astrophysics,  
Enrico Fermi Institute, University of Chicago, Chicago, Illinois 60637, U.S.A*

Self-accelerating solutions in massive gravity provide explicit, calculable examples that exhibit the general interplay between superluminality, the well-posedness of the Cauchy problem, and strong coupling. For three particular classes of vacuum solutions, one of which is new to this work, we construct the conformal diagram for the characteristic surfaces on which isotropic stress-energy perturbations propagate. With one exception, all solutions necessarily possess spacelike characteristics, indicating perturbative superluminality. Foliating the spacetime with these surfaces gives a pathological frame where kinetic terms of the perturbations vanish, confusing the Hamiltonian counting of degrees of freedom. This frame dependence distinguishes the vanishing of kinetic terms from strong coupling of perturbations or an ill-posed Cauchy problem. We give examples where spacelike characteristics do and do not originate from a point where perturbation theory breaks down and where spacelike surfaces do or do not intersect all characteristics in the past light cone of a given observer. The global structure of spacetime also reveals issues that are unique to theories with two metrics: in all three classes of solutions, the Minkowski fiducial space fails to cover the entire de Sitter spacetime allowing worldlines of observers to end in finite proper time at determinant singularities. Characteristics run tangent to these surfaces requiring *ad hoc* rules to establish continuity across singularities.

## I. INTRODUCTION

Building upon earlier work [1–3], de Rham, Gabadadze and Tolley (dRGT) [4] first constructed a consistent interacting theory of a massive spin-2 field using an auxiliary flat fiducial metric. Though the study of this theory and other nonlinear massive gravity variants has now reached a somewhat mature stage [5], there remain many outstanding questions to be addressed and understood.

Foremost amongst these is the status of cosmological solutions within the theory. The dRGT theory does not admit flat or closed cosmological solutions where the spacetime and fiducial metrics are simultaneously homogeneous and isotropic [6, 7]. Though this complicates matters computationally, it does not automatically destroy the phenomenological viability of cosmological solutions. The spacetime upon which matter fields propagate can be homogeneous and isotropic for any choice of spatial curvature [8–10]. Indeed, many explicit examples of cosmological solutions to the theory have been found where accelerated expansion occurs without a true cosmological constant [6–16].

Though these solutions are satisfactory as far as background evolution is concerned, the theory of fluctuations about these solutions is somewhat paradoxical. Analyses of perturbations about these self-accelerating backgrounds [17, 18] reveal pathologies such as unboundedness of the Hamiltonian for isotropic perturbations, or strong-coupling of degrees of freedom in specific backgrounds, but often these appear in quite a subtle way [19]. For example it has been claimed that the number of degrees of freedom identified by a Hamiltonian analysis depends on a choice of coordinates [18]. Therefore, a

worthwhile aim is to understand more fully the relationship between these potentially problematic features.

More generally, this broad class of self-accelerating solutions provides an interesting playground to explore fundamental field-theoretical questions which remain unresolved in massive gravity and beyond. In particular, there has been much recent interest in the interplay between superluminality in field theories and strong coupling phenomena, as well as what if anything the presence of these features implies about the well-posedness of the Cauchy problem (for various perspectives, see [20–39]). The self-accelerating sector of dRGT allows us an opportunity to explore these issues with explicit solutions: the theory of isotropic perturbations about these solutions turns out to be rather simple [17]. In particular, it is possible to solve exactly for the characteristic hypersurfaces upon which graviton stress energy fluctuations propagate. This makes it rather easy to study perturbative aspects of the causal structure of self-accelerating backgrounds. Therefore, another worthwhile avenue to explore is to what extent we can abstract general lessons about superluminality, strong coupling and Cauchy surfaces from these particular examples.

In this paper, we pursue both of these goals in tandem. After reviewing the structure of the dRGT theory—and in particular the construction of self-accelerating solutions of Ref. [8]—we focus on three particular families of vacuum solutions, one of which is new to this work. We explicitly solve for the characteristics for isotropic perturbations and examine their causal structure via conformal diagrams. In this sense, our study is related to the analysis of Ref. [35–40] but our exact solutions are general and do not require discontinuous or “shock” con-

ditions which automatically entail strong coupling. We find many interesting phenomena: in particular, the solutions we consider exhibit superluminal propagation of fluctuations by necessity except in one unique case, only some of which provide a well-posed Cauchy problem and originate from singular conditions where strong-coupling might reside.

Perturbative superluminality on specific backgrounds does not necessarily indicate superluminality in the full theory (see [21–23]), which would present problems for a local and Lorentz-invariant UV completion of the theory itself [20], nor does it imply acausal structures such as closed timelike curves [41, 42]. However these examples do highlight the fact that the highly related notions of superluminality, strong coupling and well-posed Cauchy problem are conceptually distinct.

Our examples also highlight an issue that is unique to a theory with two metrics. In all three families of vacuum solutions, the Minkowski fiducial space fails to cover the entire spacetime. The point at which the Minkowski chart, or unitary gauge, ends is called a determinant singularity; it is diffeomorphism-invariant and hence physical [43, 44]. In these examples, worldlines of some observers can intersect the singularity in finite proper time and for others the singularity lies in their past light cone requiring *ad hoc* rules for continuing worldlines or boundary conditions.

The paper is organized as follows. In §II, we review the construction of bi-isotropic self-accelerating background solutions [8] and isotropic perturbations around them [17]. We then specialize to the vacuum case in §III and discuss the global structure of the spacetime background and fiducial metric for three families of solutions, one of which is new to this paper. In §IV, we employ a characteristic analysis of perturbations around these backgrounds to expose the relationship between superluminality, strong coupling and the well-posedness of the Cauchy problem. We discuss the implications of these results in §V.

## II. SELF-ACCELERATION IN MASSIVE GRAVITY

In this section we briefly review the properties of the dRGT theory of massive gravity, the construction of self-accelerating background solutions, and spherically symmetric perturbations around them.

### A. Fiducial Metric

The dRGT [4] nonlinear theory of a massive spin-2 field is given by the following action which propagates only the expected 5 polarizations of a massive graviton:

$$S = \frac{M_{\text{Pl}}^2}{2} \int d^4x \sqrt{-g} \left( R - m^2 \sum_{k=0}^4 \frac{\beta_k}{k!} F_k(\gamma) \right), \quad (1)$$

where  $M_{\text{Pl}}^2 = (8\pi G)^{-1}$  is the reduced Planck mass and the  $F_k$  terms are characteristic polynomials of the matrix  $\gamma$ . These can be written explicitly as

$$\begin{aligned} F_0(\gamma) &= 1, \\ F_1(\gamma) &= [\gamma], \\ F_2(\gamma) &= [\gamma]^2 - [\gamma^2], \\ F_3(\gamma) &= [\gamma]^3 - 3[\gamma][\gamma^2] + 2[\gamma^3], \\ F_4(\gamma) &= [\gamma]^4 - 6[\gamma]^2[\gamma^2] + 3[\gamma^2]^2 + 8[\gamma][\gamma^3] - 6[\gamma^4], \end{aligned} \quad (2)$$

where  $[\ ]$  denotes the trace of the enclosed matrix. The matrix  $\gamma$  is the square root of the product of the inverse spacetime metric  $\mathbf{g}^{-1}$  and a flat fiducial metric  $\Sigma$

$$\gamma^\mu{}_\alpha \gamma^\alpha{}_\nu = g^{\mu\alpha} \Sigma_{\alpha\nu}. \quad (3)$$

The parameters of the theory defined by Eq. (1) are  $m$ —the graviton mass—and the  $\beta_k$ . These parameters are not all independent, but rather they depend on two fundamental independent parameters  $\{\alpha_3, \alpha_4\}$  through

$$\begin{aligned} \beta_0 &= -12(1 + 2\alpha_3 + 2\alpha_4), \\ \beta_1 &= 6(1 + 3\alpha_3 + 4\alpha_4), \\ \beta_2 &= -2(1 + 6\alpha_3 + 12\alpha_4), \\ \beta_3 &= 6(\alpha_3 + 4\alpha_4), \\ \beta_4 &= -24\alpha_4. \end{aligned} \quad (4)$$

The chart of the spacetime metric for which the fiducial metric is represented by the Minkowski metric  $\Sigma_{\mu\nu} = \eta_{\mu\nu}$  is called unitary gauge and there the spacetime metric possesses additional degrees of freedom compared to Einstein gravity. Diffeomorphism invariance can be restored by employing the Stückelberg trick to introduce four scalar functions,  $\phi^a$ , to represent the flat fiducial metric in arbitrary coordinates

$$\Sigma_{\mu\nu} = \eta_{ab} \partial_\mu \phi^a \partial_\nu \phi^b. \quad (5)$$

The  $\phi^a$  are equal to the unitary gauge coordinates  $x_u^\mu$  and absorb the extra polarization states in arbitrary gauges where diffeomorphism invariance is used to eliminate or constrain the metric terms. The matrix  $\partial_\mu \phi^a$  then represents the Jacobian of the coordinate transform between a general set of coordinates  $x^\mu$  and  $x_u^\mu$ .

Minkowski space may not cover, or equivalently unitary gauge may not chart, the entire spacetime; this situation is signaled by a non-invertible Jacobian transform, which we call a determinant singularity [43]. Unlike a pure coordinate singularity, a determinant singularity does not depend on the chart of the spacetime. This is because the ratio of determinants of the two metrics

$$\det(\mathbf{g}^{-1}\Sigma) = \det(\mathbf{g}_u^{-1}\eta) = -\det(\mathbf{g}_u^{-1}) \quad (6)$$

is a spacetime scalar. A coordinate singularity in the unitary chart of the spacetime metric  $\mathbf{g}_u$  therefore becomes a coordinate-invariant determinant singularity. In contrast to a curvature singularity, the two metrics need

not individually have any diffeomorphism invariant singularities, despite the fact that combined they display a determinant singularity.

Physically, the presence of two metrics means that worldlines of observers may end after a finite proper time in spacetime has elapsed, since an infinite interval can elapse as measured by the fiducial metric. This geodesic incompleteness is another indicator that we should take determinant singularities seriously. It is possible to continue worldlines past these singularities in the spacetime, but this requires multiple copies of Minkowski space and a rule for continuing the chart—or equivalently the Stückelberg fields—that is not directly imposed by the action.

## B. Background Equations of Motion

For any isotropic spacetime metric, including cosmological solutions with arbitrary matter content, there are solutions to the dRGT equations of motion where the stress-energy associated with the graviton potential in Eq. (1) behaves as a cosmological constant. The construction of Ref. [8], which we now review, is in fact extensible beyond dRGT to cases with non-flat bi-isotropic and dynamical metrics [44, 45].

Any metric with spatial slices invariant under  $SO(3)$  rotations can be written in isotropic coordinates, in which the line element takes the form

$$ds^2 = -b^2(t, r)dt^2 + a^2(t, r)(dr^2 + r^2d\Omega_2^2), \quad (7)$$

where  $d\Omega_2^2$  is the line element on a 2-sphere. If the fiducial metric is rotationally invariant in the same coordinate system (*i.e.*, the metrics are bi-isotropic), the Stückelberg fields take the following form,

$$\begin{aligned} \phi^0 &= f(t, r), \\ \phi^i &= g(t, r)\frac{x^i}{r}, \end{aligned} \quad (8)$$

and are completely specified by the two functions  $f$  and  $g$ . Note that  $f = t_u$  is the unitary gauge time and  $g = r_u$  is the unitary gauge radius that describe the fiducial flat line element

$$ds_\Sigma^2 = \Sigma_{\mu\nu}dx^\mu dx^\nu = -df^2 + dg^2 + g^2d\Omega_2^2. \quad (9)$$

Unitary gauge uniquely specifies the coordinates, whereas the isotropic condition does not, leading to multiple paths to finding the same solution and superficially different descriptions of their dynamics. Once solutions for  $f$  and  $g$  are found using any isotropic construction they may be re-expressed in an alternate choice of coordinates since both are spacetime scalars.

Upon inserting the ansätze (7) and (8) into the action (1), we find that the equation of motion for the spatial Stückelberg fields is satisfied by

$$g(t, r) = x_0 a(t, r)r, \quad (10)$$

where the constant  $x_0$  solves the polynomial equation  $P_1(x_0) = 0$  with

$$P_1(x) \equiv 2(3-2x) + 6(x-1)(x-3)\alpha_3 + 24(x-1)^2\alpha_4. \quad (11)$$

On this solution, the effective stress tensor due to the presence of the non-derivative graviton interactions takes the form of an effective cosmological constant

$$T_{\mu\nu} = -\Lambda_{\text{eff}} M_{\text{Pl}}^2 g_{\mu\nu}, \quad (12)$$

where

$$\Lambda_{\text{eff}} = \frac{1}{2}m^2 P_0(x_0), \quad (13)$$

and the polynomial  $P_0(x)$  is given by

$$\begin{aligned} P_0(x) &= -12 - 2x(x-6) - 12(x-1)(x-2)\alpha_3 \\ &\quad - 24(x-1)^2\alpha_4. \end{aligned} \quad (14)$$

Unitary time,  $f(t, r)$ , satisfies the equation

$$\sqrt{X} = \frac{W}{x_0} + x_0, \quad (15)$$

where

$$\begin{aligned} X &\equiv \left(\frac{\dot{f}}{b} + \mu\frac{g'}{a}\right)^2 - \left(\frac{\dot{g}}{b} + \mu\frac{f'}{a}\right)^2, \\ W &\equiv \frac{\mu}{ab}(\dot{f}g' - \dot{g}f'), \end{aligned} \quad (16)$$

with branches due to the matrix square root  $\gamma$  defined in Eq. (3) allowing  $\mu \equiv \pm 1$ . Here and throughout, over-dots denote derivatives with respect to  $t$  and primes denote derivatives with respect to  $r$ . Note that  $W$  is proportional to the determinant of the Jacobian transform from unitary gauge to isotropic coordinates. When  $W = \pm\infty, 0$  or is undefined because either  $f$  or  $g$  are not continuously differentiable, the Jacobian transform is not invertible. We call all of these cases a determinant singularity. Analytic continuation is sometimes possible, especially in the later two cases, but requires a second fiducial metric and solution with its own choice of branch [43]. We pick  $\mu = 1$  for the examples in the following sections.

Using Eq. (10) in Eq. (15), we see that the latter equation can be cast as

$$\begin{aligned} b^2 f'^2 + 2ar(a' \dot{f}^2 - \dot{a} \dot{f} f') + r^2(a' \dot{f} - \dot{a} f')^2 \\ = x_0^2 (a'^2 b^2 r^2 + 2a' ab^2 r - \dot{a}^2 a^2 r^2). \end{aligned} \quad (17)$$

This nonlinear partial differential equation has an infinite number of distinct self-accelerating solutions, each of which possesses the same background spacetime metric and  $\Lambda_{\text{eff}}$ . In order to specify a solution, one assumes a functional form for  $a$  and  $b$  consistent with the Einstein equations sourced by  $\Lambda_{\text{eff}}$  and the matter content and then solves Eq. (17) to determine  $f$ . In §III, we will perform this procedure, choosing  $a$  and  $b$  so that there is no matter content and the background spacetime is de Sitter.

For solutions to the equation of motion (17) which satisfy the condition

$$\dot{f}f' = \dot{g}g', \quad (18)$$

the fiducial metric Eq. (9) is also diagonal in the same  $(t, r)$  coordinates that the spacetime metric is diagonal. We shall see that this is exactly the condition for which the kinetic term of isotropic perturbations vanishes [18]. However, we can analyze the dynamics of the same solution in alternate isotropic coordinate systems which mix the temporal and radial coordinates where bi-diagonality and vanishing kinetic terms do not apply. Moreover, the diffeomorphism invariance of the Stückelberg representation means that we are not even limited to isotropic coordinate systems when analyzing the dynamics.

### C. Isotropic Perturbations

Given the rotational invariance of the background spacetime metric and Stückelberg fields, isotropic perturbations about these background solutions are straightforward to analyze (*cf.* [19]). This is a reasonable starting point, as uncovering problems in this restricted class of perturbations would already indicate a pathology of the background solution. Note that the converse is not true: a background solution with healthy isotropic perturbations can still show pathologies in the anisotropic sector.

In order to study fluctuations about the background solutions we are considering, we perturb both the metric variables and Stückelberg fields about their background values; isotropic perturbations are specified by four functions of  $(t, r)$ :  $\delta a, \delta b, \delta f$  and  $\delta g$ . Varying the quadratic action for these variables given in Ref. [17] yields an independent equation of motion for a specific combination

$$\delta\Gamma(t, r) = \delta g(t, r) - x_0 r \delta a(t, r). \quad (19)$$

This combination is special because it is precisely the variable which quantifies perturbations away from the effective cosmological constant solution; perturbations for which  $\delta\Gamma = 0$  still satisfy (10) and therefore leave  $\Lambda_{\text{eff}}$  unchanged. The equation of motion for the variable  $\delta\Gamma$  is [17]

$$\begin{aligned} \partial_t \left[ \frac{a^2 r}{\sqrt{X}} \left( \frac{\dot{f}}{b} + \mu \frac{g'}{a} \right) \delta\Gamma \right] &= \partial_r \left[ \frac{abr}{\sqrt{X}} \left( \mu \frac{\dot{g}}{b} + \frac{f'}{a} \right) \delta\Gamma \right] \\ &+ \mu a^2 r^2 \left[ \frac{(ar)'}{ar} \delta\dot{\Gamma} - \frac{\dot{a}}{a} \delta\Gamma' \right]. \end{aligned} \quad (20)$$

Equation (20) is first order in both time and space derivatives and does not depend on other perturbations. The  $\delta f$  equation of motion is also first order, but unlike the  $\delta\Gamma$  equation it requires specification of  $\delta\Gamma$  and other perturbations. To linear order in the Stückelberg fluctuations, the stress energy tensor of the perturbations depends only on  $\delta\Gamma$  and we therefore focus on its dynamics. The equation of motion (20) is equivalent to local conservation of stress energy [17].

The coefficient of the temporal derivative term,

$$A_t = \frac{a^2 r}{\sqrt{X}} \left( \frac{\dot{f}}{b} + \mu \frac{g'}{a} \right) - \mu ar(ar)', \quad (21)$$

is of special interest to the time evolution of the perturbations. In a choice of isotropic coordinates where  $A_t = 0$ , the kinetic term for  $\delta\Gamma$  vanishes and hence the equation of motion (20) does not specify the evolution of perturbations off of a constant time surface. Combining Eq. (17) and Eq. (18), we see that  $A_t = 0$  whenever the spacetime and fiducial metrics are bi-diagonal and vice versa.

When  $A_t = 0$ , the energy density, momentum and pressure associated with any  $\delta\Gamma$  fluctuation vanish to linear order [17]. Thus energy-momentum conservation, though enforced by the equation of motion, also does not yield equations that allow evolution of  $\delta\Gamma$  off of constant time surfaces. Instead, the nonvanishing anisotropic stresses must obey a constraint equation.

On the other hand, the fact that the equation of motion can be written in terms of different choices of isotropic time—or more generally different foliations of the spacetime—indicates that the vanishing of the kinetic term is a coordinate dependent statement [18].<sup>1</sup> In a choice where the kinetic term is present, the equation of motion does supply an evolution equation, or equivalently the constraint on stresses becomes a non-trivial equation for energy-momentum conservation. We shall see that this is a generic property for perturbations that propagate superluminally, *i.e.*, on spacelike characteristics.

Relatedly, Ref. [18] show through a Hamiltonian analysis that the number of propagating (isotropic) degrees of freedom in a given isotropic frame is one if  $A_t \neq 0$  and zero if  $A_t = 0$ . The number of degrees of freedom counted in this way, therefore depends on the coordinate system. For  $A_t = 0$ , the Hamiltonian is not associated with the time evolution of the system, in the sense that it defines evolution along a spatial slice, rather than transverse to it. As such, it is somewhat unclear how to interpret the Hamiltonian analysis in this case. Further, in the case  $A_t \neq 0$ , the canonical momentum for  $\delta\Gamma$  appears linearly in the Hamiltonian, and thus the Hamiltonian is unbounded from below.

### III. VACUUM SOLUTIONS

In this section we specialize to background solutions without any matter content. In these solutions the only source of stress-energy determining the background is the effective cosmological constant,  $\Lambda_{\text{eff}}$ , and the spacetime

<sup>1</sup> Note that there are more prosaic examples of this phenomenon: a scalar field with a superluminal phase velocity considered in an appropriately Lorentz-boosted frame will have a vanishing kinetic term [20].

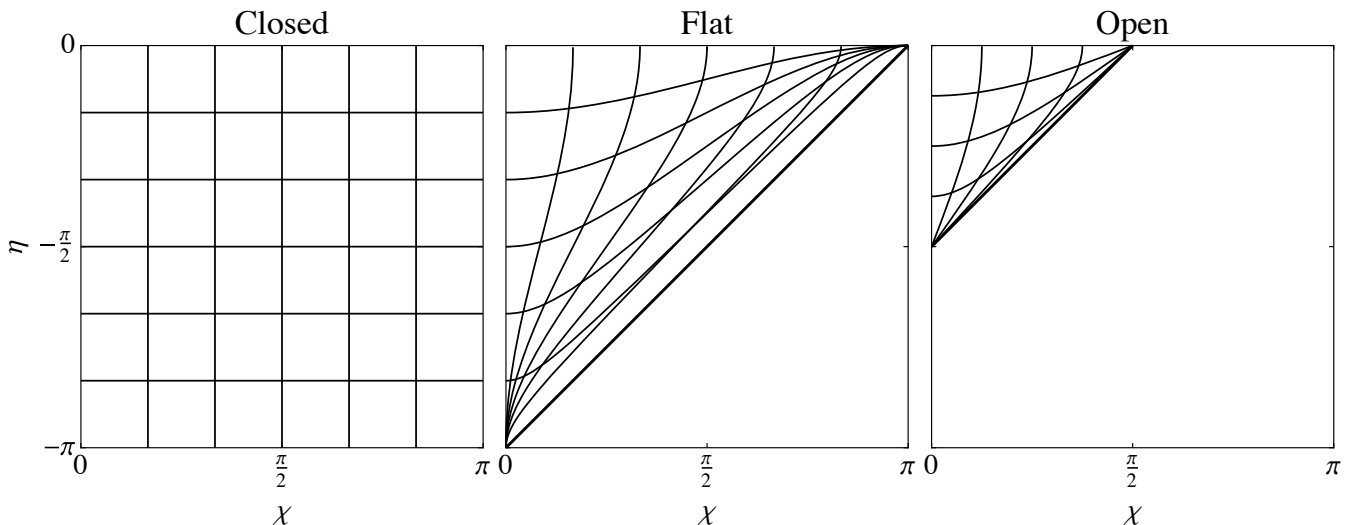


FIG. 1. Conformal diagrams showing portions of de Sitter space charted by closed (left), flat (middle) and open (right) foliations. Thick lines indicate coordinate singularities. Superimposed are lines of constant isotropic time and radius for each foliation.

metric describes a de Sitter space. We first discuss the conformal and three isotropic charts of the de Sitter space that play a prominent role in both the construction of solutions and the investigation of their global properties. We then turn to three families of self-accelerating solutions and discuss their global structure, namely the appearance of their determinant singularities.

### A. De Sitter Charts

One special feature of de Sitter space is that there is no preferred temporal coordinate to define a foliation with respect to. Sections of the full spacetime can therefore be charted by isotropic coordinates where the constant time slices have positive, negative or zero spatial curvature. The conformal diagram for de Sitter space can be constructed from the positive curvature (closed) foliation of the spacetime, where the line element takes the form

$$ds^2 = \left( \frac{1}{H \sin \eta} \right)^2 (-d\eta^2 + d\chi^2 + \sin^2 \chi d\Omega_2^2), \quad (22)$$

with the dimensionless conformal time  $\eta \in (-\pi, 0)$  and the comoving radial coordinate  $\chi \in [0, \pi]$ . Here  $H^2 = \Lambda_{\text{eff}}/3$ . We use the  $(\eta, \chi)$  conformal diagram throughout to represent the spacetime.

Closed, flat, and open isotropic coordinates can alternately be used to foliate portions of de Sitter space and are useful in finding solutions to the background massive gravity equations and for investigating perturbations. With the transformations

$$\begin{aligned} \sinh(Ht_c) &= -\cot \eta, \\ Hr_c &= 2 \tan(\chi/2), \end{aligned} \quad (23)$$

the line element (22) takes its closed isotropic form

$$ds^2 = -dt_c^2 + \left[ \frac{\cosh(Ht_c)}{1 + (Hr_c)^2/4} \right]^2 (dr_c^2 + r_c^2 d\Omega_2^2), \quad (24)$$

where  $t_c \in (-\infty, \infty)$ ,  $r_c \in [0, \infty)$ . These coordinates chart the entire de Sitter spacetime. Similarly, defining the coordinates

$$\begin{aligned} e^{Ht_f} &= -\frac{\cos \chi + \cos \eta}{\sin \eta}, \\ Hr_f &= \frac{\sin \chi}{\cos \chi + \cos \eta}, \end{aligned} \quad (25)$$

obtains the flat isotropic form

$$ds^2 = -dt_f^2 + e^{2Ht_f} (dr_f^2 + r_f^2 d\Omega_2^2), \quad (26)$$

where  $Ht_f \in (-\infty, \infty)$ ,  $Hr_f \in [0, \infty)$ . These coordinates chart the upper left half of the conformal diagram  $\eta > \chi - \pi$ . Finally, the coordinate definition

$$\begin{aligned} \ln [\tanh(Ht_o/2)] &= \tanh^{-1} \left( \frac{\sin \eta}{\cos \chi} \right), \\ 2 \tanh^{-1}(Hr_o/2) &= \tanh^{-1} \left( \frac{\sin \chi}{\cos \eta} \right), \end{aligned} \quad (27)$$

gives the open isotropic form

$$ds^2 = -dt_o^2 + \left[ \frac{\sinh(Ht_o)}{1 - (Hr_o)^2/4} \right]^2 (dr_o^2 + r_o^2 d\Omega_2^2), \quad (28)$$

where  $Ht_o \in (0, \infty)$ ,  $Hr_o \in [0, 2)$ . These coordinates chart the upper left wedge of the conformal diagram  $\eta > \chi - \pi/2$ , corresponding to 1/8 of the space. We display these charts with the curves of constant  $t_i$  and  $r_i$  in Fig. 1.

Self-accelerating background solutions appear superficially different in different isotropic coordinates. More

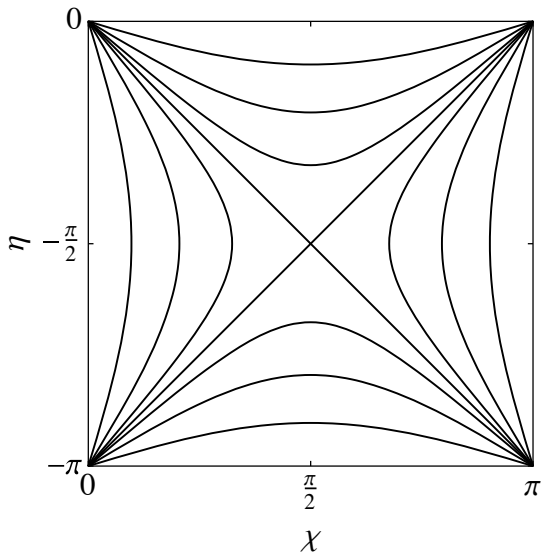


FIG. 2. Constant unitary gauge radius  $g$  curves, given by Eq. (29). These are common to all bi-isotropic solutions.

importantly, differences in the constant time surfaces cause the kinetic terms for the perturbations to appear differently in each case, as emphasized by Ref. [18]. Of course, the causal structure of the conformal diagram remains unchanged and serves to highlight the spacelike, timelike or lightlike nature of curves rather than coordinate dependent definitions of simultaneity. For this reason, it will be convenient to plot characteristics on the conformal diagram.

## B. Explicit Solutions

We now combine the isotropic de Sitter charts with the formalism of §II B to construct vacuum solutions to the massive gravity equations of motion.

### Radial solution: $g$ and equations of motion

Since closed isotropic coordinates chart the whole spacetime, it is convenient to use these coordinates to find self-accelerating solutions. Using the closed line element Eq. (24) in the radial unitary gauge solution of Eq. (10), we obtain

$$g = x_0 \frac{\cosh(Ht_c)}{1 + (Hr_c)^2/4} r_c = -\frac{x_0 \sin \chi}{H \sin \eta}. \quad (29)$$

Fig. 2 shows the contours of constant  $g$  in the conformal diagram. As the conformal diagram makes obvious,  $g$  is 4-fold symmetric in the de Sitter spacetime since  $\eta \rightarrow -\pi - \eta$  and/or  $\chi \rightarrow \pi - \chi$  provide the same values.

We then look for a choice of unitary time  $f$  that solves Eq. (17), which in the coordinates (22) takes the explicit

form

$$\begin{aligned} & (f_{,\chi}^2 \cot^2 \chi - f_{,\eta}^2) \sin^2 \eta + f_{,\chi}^2 + f_{,\chi} f_{,\eta} \cot \chi \sin(2\eta) \\ & = -\frac{x_0^2}{H^2} \csc^2 \eta. \end{aligned} \quad (30)$$

Below we consider three explicit families of solutions to Eq. (30), corresponding to different self-accelerating backgrounds whose perturbations we will examine in the subsequent sections.

As an aside, we note that (30) can be cast in a particularly simple form,

$$f_{,\tau}^2 - f_{,\rho}^2 = \frac{x_0^2}{H^2}, \quad (31)$$

by a further coordinate transform [46]

$$\rho = \frac{\cos \chi}{\sin \eta}, \quad \tau = -\cot \eta, \quad (32)$$

with  $\tau \in (-\infty, \infty)$ ,  $\rho \in (-\infty, \infty)$ .

### Open solution: $f_o$

The simple ansatz that  $f$  is a function of  $\eta$  alone leads to the solutions first identified in Ref. [7] through an open slicing construction, where  $f$  is given by

$$f_o(\eta, \chi) = -\frac{x_0}{H} \cot \eta. \quad (33)$$

In open slicing, the spacetime and fiducial metrics are bi-diagonal (because Eq. (18) is satisfied) and manifestly homogeneous and isotropic. This property of open slicing applies beyond the de Sitter solutions considered here to a general FRW spacetime, giving this solution a special status. As pointed out by Ref. [18], and rediscovered by Ref. [46], bi-diagonality does not hold in the closed or flat slicings of de Sitter. However, the ability to define multiple homogeneous and isotropic slicings and threadings of the spacetime is special to de Sitter. For a general FRW spacetime, this freedom no longer exists since the homogeneity of an evolving background density picks out a unique time slicing.

Curves of constant unitary gauge time for this solution are plotted in Fig. 3. Note that the coordinate pair  $(f_o, g)$  maps to two different  $(\eta, \chi)$  points in the spacetime related by  $\chi \rightarrow \pi - \chi$  and correspondingly the determinant of the Jacobian transformation to unitary gauge is zero along  $\chi = \pi/2$ . Therefore, more than one copy of the Minkowski fiducial space is required to cover the entire spacetime. For this solution, the singularity lies in the past light cone of an observer at  $\chi = 0$  and hence boundary conditions that represent the continuation with a second fiducial metric are required. Note that—as mentioned in §II—such a rule for continuation is *ad hoc* as it must be imposed by hand.

### Stationary solution: $f_C$

Self-accelerating solutions where the spacetime metric in unitary gauge is stationary were first identified in

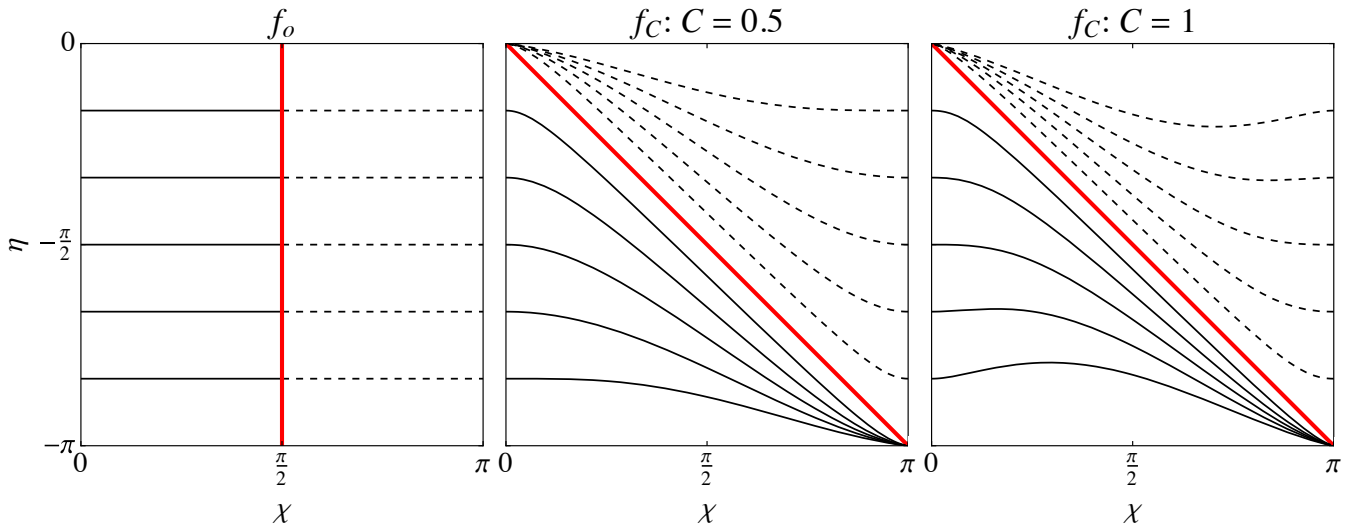


FIG. 3. Constant unitary time curves for various well-known self-accelerating solutions: open  $f_o$  (left), and stationary  $f_C$  for  $C = 1/2$  (middle) and  $f_C$  for  $C = 1$  (right). Solid lines indicate constant unitary time slices extending from  $\chi = 0$  which end at a determinant singularity (red lines). Dashed lines indicate an extension of solutions with a second copy of the fiducial metric.

Ref. [13]. In conformal coordinates, unitary time takes the form

$$f_C = \frac{x_0}{CH} \left( \ln \left| \frac{C^2 e^{Ht_f}}{1-y} \right| - y \right),$$

$$y = \sqrt{1 + C^2(\sin^2 \chi / \sin^2 \eta - 1)}, \quad (34)$$

where  $C \in (0, 1]$  is a free parameter,  $y \in [0, \infty)$ , and  $t_f(\chi, \eta)$  is the extension of flat isotropic time to the full de Sitter space using Eq. (25). The coordinate pair  $(f_C, g)$  maps to two spacetime points  $(\eta, \chi)$  and  $(-\pi - \eta, \pi - \chi)$ . The inversion singularity thus is at  $\chi = -\eta$  and is characterized by a divergence in unitary time  $f_C \rightarrow \infty$  which prevents its differentiability. Again, two copies of the Minkowski fiducial space are required to cover the spacetime. In this case, the singularity is along the past light cone of the observer at  $\chi = 0$  at the terminal conformal time  $\eta = 0$ . Conformal diagrams showing curves of constant  $f_C$  for  $C = 1/2$  and  $C = 1$  are plotted in Fig. 3.

A different construction of this solution that starts in static de Sitter coordinates [46] is in fact equivalent to Eq. (34) after relating their parameter  $q$  to  $C$  as  $q^2 = 1/C^2 - 1$ . The equivalence between the two classes of solutions can also be seen directly in the construction itself since Ref. [13] showed that stationary unitary coordinates and static de Sitter coordinates are simply related by a radially dependent offset to the static time coordinate.

#### New solution: $f_{ab}$

Finally, we can generalize a particular solution introduced in Ref. [18], to a new two parameter class, where the temporal Stückelberg field takes the following form

$$f_{ab} = \pm \frac{x_0}{H} \sqrt{(a - \cot \eta)^2 - (b - \cos \chi \csc \eta)^2}. \quad (35)$$

Here, the parameters  $a, b$  can take on any real value except for  $a = b = 0$ . For that case, we have  $f_{00}^2 = g^2 - (x_0/H)^2$ , such that unitary time and radius cannot identify a unique spacetime point. Ref. [18] previously considered the case of  $a = 0, b = 1$ .

In the full spacetime  $f_{ab}$  is not guaranteed to be real and so unitary gauge ends in a determinant singularity where  $W = \pm\infty$ . Approaching this point, the change in unitary time (or proper time measured by the fiducial metric) per unit conformal time (or proper time measured by the spacetime metric) diverges. Unlike the case of  $W = 0$ , an analytic continuation of unitary coordinates would make a copy of the fiducial metric with a Riemannian rather than Lorentzian signature. Thus, unlike the other solutions, it does not appear that  $f_{ab}$  can be continued beyond this type of determinant singularity with copies of the fiducial metric in the same class of solutions.

Changing the sign of  $a$  reflects solutions vertically across  $\eta = -\pi/2$  whereas changing the sign of  $b$  reflects horizontally across  $\chi = \pi/2$ . The determinant singularities  $W = \pm\infty$  occur where  $f_{ab} = 0$  and bound regions past which the solutions cannot be continued within the class. These singularities intersect at

$$\cot \eta = a, \quad \cos \chi = -\frac{b}{\sqrt{1+a^2}}, \quad (36)$$

if  $|b| \leq \sqrt{1+a^2}$ . The  $W = 0$  singularity occurs along the curve  $a \cos \chi = b \cos \eta$  and intersects both  $W = \pm\infty$  singularities at their crossing point.

We show several examples from this class in Fig. 4. Displacing  $b$  from zero at  $a = 0$  breaks the  $\chi$  or left-right symmetry of the conformal diagram allowing constant unitary time surfaces to foliate the spacetime near one

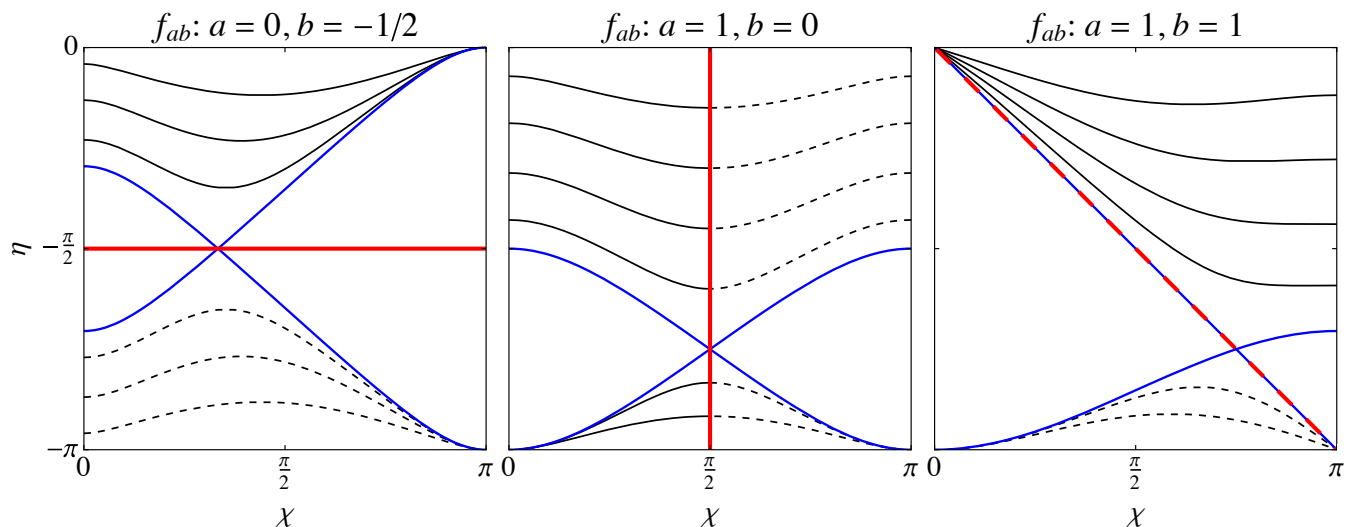


FIG. 4. Constant unitary time curves for the new  $f_{ab}$  class of self-accelerating solutions. In addition to the zero determinant singularity (thick red lines) there also appear singularities where the determinant is infinite (blue lines), in the  $a = b = 1$  case the two coincide. Across the infinite determinant singularity, a naïve analytic continuation would require a Riemannian rather than Lorentzian second fiducial metric.

pole with the other pole hidden behind a  $W = \pm\infty$  determinant singularity. The unbroken  $\eta$  or top-bottom symmetry has a corresponding  $W = 0$  singularity at  $\eta = -\pi/2$  across which solutions can be extended with a second fiducial metric. Displacing  $a$  from zero at  $b = 0$  does the converse, allowing constant unitary time surfaces to foliate the spacetime near both poles at either the top or bottom sections of the diagram with a  $W = 0$  singularity at  $\chi = \pi/2$ , again with a second branch of the solution across it. Displacing both equally makes one of the  $W = \pm\infty$  curves coincide with  $W = 0$ , allowing foliation around only one pole and only on the top or bottom section.

### C. Determinant Singularities

All three families of solutions exhibit determinant singularities. Worldlines of observers can intersect these singularities in the bulk of the spacetime, *i.e.*, after only a finite amount of proper time has elapsed. For other observers, the singularity lies in the past light cone. Both properties imply that the incompleteness of the solutions there cannot simply be ignored.

In the open  $f_o$  solution, a naïve continuation past the  $W = 0$  singularity keeps the Stückelberg fields or unitary gauge coordinates continuous and differentiable but multivalued. In the static  $f_C$  solution, naïve continuation keeps them continuous but not differentiable at the singularity. In the new  $f_{ab}$  solutions, naïve continuation beyond the  $W = \pm\infty$  singularities is not possible and when they intersect at a specific point in the spacetime bulk they do so at the  $W = 0$  singularity.

Finally, by pushing the  $W = \pm\infty$  singularities of the

$f_{ab}$  case to the top or bottom of the conformal diagram it can be made to resemble the  $f_o$  and  $f_C$  solutions. The  $f_o$  solution picks out the same unitary time surfaces as the limiting case of  $a \rightarrow \infty$ ,  $b = 0$  since  $f_o$  and  $f_{ab}$  are then linearly related. Likewise, the  $a = b \rightarrow \infty$  limit of  $f_{ab}$  leads to the same surfaces of constant unitary time as the  $f_C$  solution for  $C \rightarrow 0$  in the upper right portion of the conformal diagram, although in this case  $f_{ab}$  is a more general function of  $f_C$ . The second copy of  $f_C$  for  $C \rightarrow 0$  in the lower left corresponds similarly to  $a = b \rightarrow -\infty$ .

As we shall see in the next section, the appearance of these singularities influences the characteristic curves on which information about perturbations propagate.

## IV. PERTURBATION CHARACTERISTICS

In this section we use the method of characteristics to explicitly solve the equation of motion (20) for the field fluctuation  $\delta\Gamma$  in the three families of background solution studied in §III B. The characteristic curves of this linear differential equation define hypersurfaces along which spherically symmetric stress-energy perturbations propagate. The conformal diagram of the curves exemplifies the difference between superluminality, strong coupling, and the well-posedness of the Cauchy problem.

### A. Method of Characteristics

We can solve the  $\delta\Gamma$  equation of motion for perturbations propagating on the background solutions using the method of characteristics. The characteristic curves of this equation also clarify the causal structure of solu-



tions. Transforming Eq. (20) from isotropic coordinates to the conformal coordinates  $(\eta, \chi)$  leads to a differential equation of the form

$$V_\eta \delta\Gamma_{,\eta} + V_\chi \delta\Gamma_{,\chi} + A \delta\Gamma = 0. \quad (37)$$

Here,

$$\begin{aligned} V_\eta &= f_{,\chi} - \tan \chi \tan \eta f_{,\eta}, \\ V_\chi &= f_{,\eta} + (\cot \chi + \csc^2 \eta \tan \chi) \tan \eta f_{,\chi}. \end{aligned} \quad (38)$$

This equation depends on the particular background  $f(\eta, \chi)$  around which we perturb and describes propagation of the  $\delta\Gamma$  perturbations in the regions of de Sitter space where  $f$  is defined. While  $A(\eta, \chi)$  is not important for the construction of characteristics themselves, it does enter into determining the field profile for  $\delta\Gamma$  along the characteristics. For completeness, it is given by

$$\begin{aligned} \frac{A}{N} &= \sin \eta \left[ \csc \eta \left( \frac{V_\eta}{N} - R_\eta \right) \right]_{,\eta} \\ &+ \cos^2 \frac{\chi}{2} \left[ \sec^2 \frac{\chi}{2} \left( \frac{V_\chi}{N} - R_\chi \right) \right]_{,\chi}, \end{aligned} \quad (39)$$

where

$$\begin{aligned} R_\eta &= \frac{\mu}{2} \cos \chi \sin^2 \chi \cot \frac{\chi}{2} \csc \eta, \\ R_\chi &= \mu \cos^2 \frac{\chi}{2} \sin^2 \chi \cot \eta \csc \eta, \\ N &= \csc^2 \chi \sec \chi \tan \chi \left[ 2\mu \cos \eta \tan \frac{\chi}{2} f_{,\chi} \right. \\ &\left. + \sec^2 \frac{\chi}{2} \left( \mu \cos \chi \sin \eta f_{,\eta} - \frac{x_0}{H} \right) \right]. \end{aligned} \quad (40)$$

The most general solution to Eq. (37) can be found from its characteristics, which are integral curves for the vector field

$$\mathbf{V} = (V_\eta, V_\chi), \quad (41)$$

with the first component in the  $\eta$  direction. Information from boundary conditions on  $\delta\Gamma$ , specified on a surface that intersects the characteristic curves, propagates along those curves to provide the general solution in the bulk. Thus conformal diagrams of characteristic curves for particular background solutions present a succinct way of describing their casual structure. In particular, the characteristic curves are

$$\begin{aligned} \text{timelike : } & |V_\eta| > |V_\chi|, \\ \text{lightlike : } & |V_\eta| = |V_\chi|, \\ \text{spacelike : } & |V_\eta| < |V_\chi|. \end{aligned} \quad (42)$$

Since Eq. (37) is a first order differential equation, the characteristic analysis yields complete solutions for  $\delta\Gamma$ , including both smooth and discontinuous cases. This should be contrasted with a characteristic analysis of a second order differential equation where in most cases the characteristics only describe the propagation of discontinuous fronts. Once a solution for  $\delta\Gamma$  is specified from boundary data in the conformal coordinate system it can be expressed in any coordinate system since it transforms as a scalar function in spacetime.

## B. Explicit Solutions

We now apply this formalism to the explicit background solutions derived in §III B and identify the characteristic curves upon which isotropic stress-energy perturbations propagate.

**Open solution:  $f_o$**

For the  $f_o$  background solution (33), the general solution given by the characteristics is

$$\begin{aligned} \delta\Gamma_o(\eta, \chi) &= \frac{\sin^2 \eta}{\sin^2 \chi} F(\phi_o), \\ \phi_o(\eta, \chi) &= \cos \chi / \sin \eta, \end{aligned} \quad (43)$$

where  $F$  is a completely arbitrary function of its argument  $\phi_o$ . Curves of  $\phi_o = \text{const.}$ , shown in Fig. 5 (left), are the characteristics of the equation and comparison with Eq. (27) shows that they coincide with constant open time  $t_o = \text{const.}$  surfaces in the wedge charted by the open coordinates. Correspondingly, in open isotropic coordinates, Eq. (20) loses its kinetic term ( $A_{t_o} = 0$ ) indicating that initial conditions at  $t_o = \text{const.}$  do not propagate off that surface. Open time slices therefore are disconnected, leading to an unspecified evolution of  $\delta\Gamma$ . In particular, information propagates instantaneously along the characteristics as measured by open time. This behavior does not violate local conservation of energy and momentum since they are both zero for any  $\delta\Gamma_o$  in these coordinates [17].

In flat or closed coordinates, these features take a superficially different form. Characteristics are still spacelike but the finite stress components in open coordinates transform to energy and momentum. This energy-momentum is conserved by the solution (43) as a consequence of Eq. (20). As discussed in §II C, this conservation law is the transformation of the constraint on the spatial stresses in open coordinates.

On the other hand, the stress-energy emanates from  $\chi = 0$  where the spatial profiles of the  $\delta\Gamma_o$  solutions diverge. Although it is not manifest in the linearized treatment from the quadratic Lagrangian, generically one might expect perturbation theory to break down here with higher order interactions making the fluctuations strongly coupled. This class of solution was excluded by the analysis of Ref. [47] by implicitly demanding regularity at  $\chi = 0$ , leading to their conclusion that the Stückelberg fields contained no degrees of freedom. Our characteristic analysis makes this assumption explicit: it corresponds to assigning boundary conditions on the timelike  $\chi = 0$  curve. More generally, there is no spacelike Cauchy surface at all in the open wedge, since a surface must be timelike to intersect all characteristics. The lack of a spacelike Cauchy surface is diffeomorphism invariant. Thus, even in flat or closed slicing, counting degrees of freedom according to initial data would lead to the conclusion that the  $f_o$  case does not possess a degree of freedom that admits a well-posed Cauchy problem. The spacetime defined by the solution  $f_o$  is an example

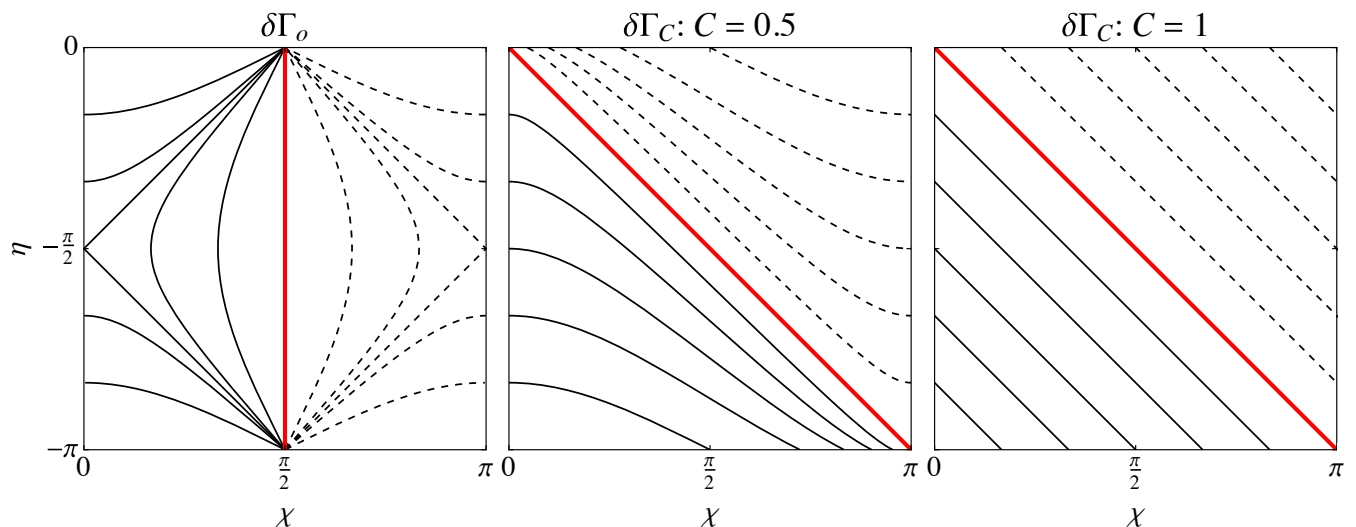


FIG. 5. Characteristic curves of  $\delta\Gamma$  for the background solutions shown in Fig. 3. For  $\delta\Gamma_o$ , characteristics coincide with constant open time curves in the open wedge of Fig. 1 and no spacelike surface intersects all characteristics. For  $\delta\Gamma_{1/2}$ , characteristics are also spacelike but those within the past light cone at  $\chi = 0$  do all intersect the spacelike surface  $\eta = -\pi$ . For the special case of  $\delta\Gamma_1$ , the characteristics are all lightlike. Red lines divide the characteristics on either side of the determinant singularity.

of a spacetime that is not globally hyperbolic.<sup>2</sup>

While imposing a regular boundary at  $\chi = 0$  for these characteristics might seem reasonable in the open wedge itself, it is interesting to track characteristics intersecting this boundary in different parts of the de Sitter space. Fig. 5 (left) shows that in the lower left wedge, where the characteristics are mirror images of the open wedge, there is a spacelike Cauchy surface at  $\eta \rightarrow -\pi$  despite superluminality, but the characteristics end rather than begin at  $\chi = 0$ . Stress-energy on a characteristic then flows into the origin requiring a boundary condition or nonlinear completion of the theory to specify its further evolution. Thus non-singular behavior on the open wedge at  $\chi = 0$  may require special initial conditions in the lower left wedge. On the other hand this behavior is analogous to collapse of a perfectly spherically symmetric density shell in ordinary linearized, Newtonian gravity. The finite angular momentum of generic perturbations may prevent singular behavior—we leave investigation of this possibility to future work. In any case, while the inwardly directed characteristics might signal strong-coupling at  $\chi = 0$  where the fluctuations diverge, like a black-hole nothing emanates classically from this point within the lower left wedge.

Interestingly, in the central diamond the  $\delta\Gamma_o$  characteristics are timelike, or subluminal, and admit a well-posed Cauchy problem. However, the characteristics are split by the determinant singularity into left and right halves.

Although information in  $\delta\Gamma_o$  never crosses this singularity in the linearized theory, the worldlines of other particles can. From the perspective of a massive gravity theory with only one copy of the fiducial metric, the determinant singularity appears as another spatial boundary condition. Even allowing the theory to be extended, the boundary condition must be imposed by hand at each order in perturbation theory, *e.g.*, by demanding that the Stückelberg fields are smooth across the boundary to the second copy of the fiducial metric [43].

#### Stationary solution: $f_C$

The characteristics of perturbations around the  $f_C$  backgrounds share some, but not all, of the properties of the  $f_o$  background. Here Eq. (37) is solved by

$$\delta\Gamma_C(\eta, \chi) = \frac{\sin^2 \eta F(\phi_C)}{\sin^2 \chi y(\eta, \chi)},$$

$$\phi_C(\eta, \chi) = \frac{\sin \eta [1 - y(\eta, \chi)]}{\cos \chi + \cos \eta}, \quad (44)$$

where  $F$  is again an arbitrary function of its argument and  $y$  was defined in Eq. (34). In Fig. 5 (mid), we show the  $\phi_C = \text{const.}$  curves for  $C = 1/2$ . These characteristics are spacelike across the whole spacetime. Even though  $\phi_C = \text{const.}$  does not coincide with the open, flat or closed choice of isotropic time, these surfaces foliate the spacetime. Thus in principle we could define a new choice of time  $t_C = \phi_C$  for which the kinetic term for  $\delta\Gamma_C$  vanishes, just like it does for  $\delta\Gamma_o$  in the open slicing. With this choice of time coordinate, information along the characteristics again propagates instantaneously and energy-momentum conservation becomes a spatial constraint.

On the lower left half of the  $\delta\Gamma_C$  diagram, the causal structure resembles the lower left wedge of the  $\delta\Gamma_o$  case.

<sup>2</sup> The existence of such a pathological spacetime as a solution to dRGT does not imply pathologies inherent to the theory itself; indeed, general relativity admits solutions which are not globally hyperbolic.

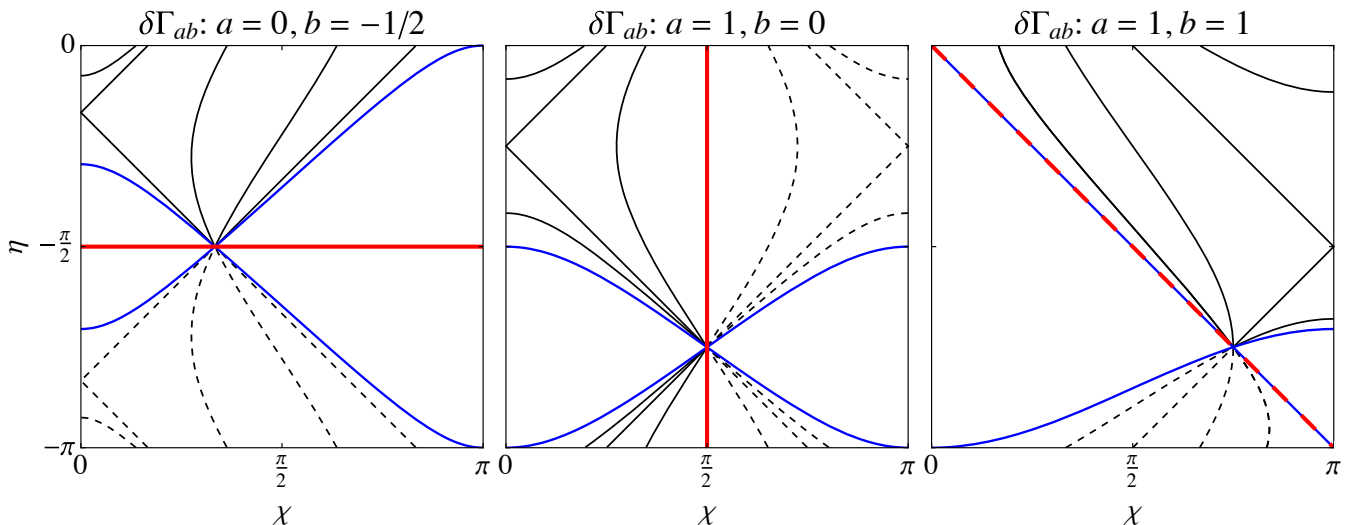


FIG. 6. Characteristic curves of  $\delta\Gamma_{ab}$  for the new class of  $f_{ab}$  solutions illustrated in Fig. 4. The determinant singularities strongly influence the causal structure of the characteristics. These backgrounds share many of the features of the  $f_o$  and  $f_C$  spacetimes discussed in Fig. 5 and provide new ones due to the  $W = \pm\infty$  determinant singularities (blue curves).

Here  $\eta \rightarrow -\pi$  provides a spacelike Cauchy surface and the characteristics end at  $\chi = 0$  with a divergent  $\delta\Gamma_{1/2}$  radial profile. On the upper right half, the structure resembles the open wedge of  $\delta\Gamma_o$  with characteristics emanating from the other pole of the closed de Sitter space. However, the two halves are divided by the null line that designates the determinant singularity where  $f$  is not continuously differentiable. Thus the outgoing characteristics of upper right half are not within the past light cone at  $\chi = 0$  unlike the  $\delta\Gamma_o$  case. This example illustrates that superluminality, a well-defined Cauchy problem, and singular field profiles in the past that might indicate problems originating from a point of strong coupling are not one-to-one related.

In the special case of  $C = 1$ ,  $y = -\sin \chi / \sin \eta$  and the characteristics of  $\delta\Gamma_1$  become null (see Fig. 5 and Ref. [17]). This special case was interpreted by Ref. [13] as having no vector in the background, based on a decoupling limit analysis. Although this choice eliminates the superluminality found in other solutions, the lightlike determinant singularity still exists for this case. While it only occurs on the past lightcone of the observer at  $\chi = 0$ ,  $\eta = 0$ , it would be within the past light cone at other points in the spacetime and still require null boundary conditions to define global solutions. Likewise other observers in the lower left region would reach the determinant singularity after finite proper time. Even with solutions continued beyond the singularity these observers would begin to cross characteristics for which no spacelike Cauchy surface exists.

**New solution:**  $f_{ab}$

For the new class of  $f_{ab}$  backgrounds, the general so-

lution is

$$\begin{aligned} \delta\Gamma_{ab}(\eta, \chi) &= \frac{\csc^2 \chi \sin^3 \eta}{\cos \eta - a \sin \eta} F(\phi_{ab}), \\ \phi_{ab}(\eta, \chi) &= \frac{\cos \chi - b \sin \eta}{\cos \eta - a \sin \eta}. \end{aligned} \quad (45)$$

This solution serves to illustrate that the nature of the characteristics is strongly influenced by the global structure of the determinant singularities discussed in §III B. Characteristics run tangent to these singularities as information in the perturbations cannot cross these curves (see Fig. 6). If  $|b| < \sqrt{1+a^2}$ , the  $W = \pm\infty$  and  $W = 0$  singularities intersect within the spacetime bulk at a point given by Eq. (36). Though the characteristics tangent to these singularities also intersect, the perturbation amplitude  $\delta\Gamma_{ab}$  diverges at this point and hence marks a point where strong coupling is likely.

Null lines that emanate from this point serve as separators which divide regions of super- and subluminal propagation much like the  $f_o$  case. This family of examples shows that these null lines are not necessarily related to special curves in the open, closed or flat de Sitter slicing. Where these null lines intersect the poles, the characteristics change from ingoing into the pole, which can be all be intersected by a single spacelike Cauchy surface in the past, to outgoing which cannot. For the special case that  $|a| = |b|$  one of these null lines coincides with the determinant singularity.

### C. Superluminality and Bi-Isotropy

In all but one example ( $\delta\Gamma_C$  with  $C = 1$ ), the characteristics intersect the poles  $\chi = 0, \pi$  at right angles at all but a finite number of points. In conformal coordinates,

perturbations propagate instantaneously there. As we now show, this is a generic property of bi-isotropic solutions. In our explanation we focus only on the  $\chi = 0$  pole as treatment of the other pole is analogous. Expanding unitary time around  $\chi = 0$  in a series

$$f(\eta, \chi) = h_0(\eta) + h_1(\eta)\chi + h_2(\eta)\chi^2 + \mathcal{O}(\chi^3) \quad (46)$$

and using the  $\chi$  expansion of the equation of motion (30), one can show that  $h_1$  is always identically zero. Physically this means that the bi-isotropy condition and the ability to make arbitrary Lorentz boosts in the fiducial space ensures that unitary time and conformal time can be locally aligned. The difference between surfaces of unitary time and conformal time thus grow at most quadratically with the distance to the pole  $\chi^2$  or more generally differ only by the curvature corrections to a locally flat spacetime metric. Since the same is true between conformal time and closed, flat, or open isotropic time, instantaneous propagation in conformal coordinates implies instantaneous propagation in isotropic coordinates at the poles. In fact, the arguments below for the generality of spacelike characteristics apply beyond the vacuum cases considered here to spacetime metrics that are locally flat near the bi-isotropy point.

Expanding the vectors defined by Eq. (38) in the same fashion,

$$\mathbf{V} = \begin{pmatrix} \mathcal{O}(\chi) \\ 2h_2 \tan \eta + h_{0,\eta} + \mathcal{O}(\chi) \end{pmatrix}. \quad (47)$$

In a neighborhood of a general point  $(\eta_0, 0)$  the leading order terms are finite and the vector field  $\mathbf{V}$  is aligned with the curves of constant conformal time  $\eta$ , signaling instantaneous propagation. Using the expansion of the background equation of motion (30), it is possible to relate  $h_2$  and  $h_{0,\eta}$  to prove that infinite superluminality at the given point is avoided if and only if

$$h_{0,\eta}(\eta_0) = \pm \frac{x_0}{H \sin \eta_0}. \quad (48)$$

As seen with our examples, this condition can be satisfied for all  $\eta$  ( $\delta\Gamma_C$  with  $C = 1$ ) or at a discrete set of points ( $\delta\Gamma_o$  and typical  $\delta\Gamma_{ab}$ ).

In fact, for the special points  $\eta_0$  at which this condition is satisfied, the characteristics are always luminal, never subluminal. Expanding  $f$  to third order in  $\chi$  allows  $\mathbf{V}$  to be expanded into linear order in both  $\chi$  and  $\eta - \eta_0$ . With repeated use of the equation of motion (30) we then find that each characteristic curve hitting  $\chi = 0$  at  $\eta_0$  is luminal. For  $h_3(\eta_0) = 0$  there are two such characteristic curves—one incoming and one outgoing—forming the typical luminal separatrices we see in Fig. 5 (left) and 6. Even for these cases, the characteristics are superluminal at all but a finite number of points. For  $h_3(\eta_0) \neq 0$ , there is only one characteristic which is either incoming or outgoing, depending on the sign of  $h_{0,\eta}/h_3$ . The  $C = 1$  example of Fig. 5 (right) exhibits a unitary time solution

$f_1$  with these very special properties. Together with solutions trivially related by  $f \rightarrow -f$  and/or  $\eta \rightarrow -\pi - \eta$ , it is in fact the unique bi-isotropic vacuum solution that evades superluminality entirely as can be shown by integrating the equation of motion (30) from the boundary conditions (48) along null coordinates.

## V. DISCUSSION

We have investigated the causal structure of three families of vacuum solutions in dRGT massive gravity. In particular, we have constructed the conformal diagram of characteristic hypersurfaces for isotropic stress-energy perturbations around these backgrounds by exploiting the first-order structure of their equation of motion. These examples provide fertile ground for studying the interplay between superluminality, an ill-posed Cauchy problem, and strong coupling as well as issues that arise for the global structure of spacetime in a theory with two metrics.

The  $f_o$  solution of Ref. [7] manifests aspects of all of these issues. This solution is distinguished because in open slicing both the background spacetime and fiducial metric are simultaneously homogeneous and isotropic. In this slicing, the kinetic term of perturbations vanishes, which was taken as an indication of possible problems with strong coupling [47]; this is supported by instabilities identified around anisotropic backgrounds [48], and the lack of an isotropic degree of freedom identified by a Hamiltonian analysis [18]. However, its kinetic term and Hamiltonian degrees of freedom only vanish in open slicing [18].

Our characteristic analysis clarifies these issues. Absence of a kinetic term in the quadratic action in a particular choice of slicing indicates instantaneous propagation of perturbations in the given frame and more generally perturbative superluminality or spacelike characteristics in any frame. The Hamiltonian analysis fails in the pathological choice of slicing along characteristics since the Hamiltonian is no longer associated with time evolution. Energy-momentum conservation likewise becomes a spatial constraint equation, confusing the counting of degrees of freedom. While it is the easiest of the inter-related issues to diagnose, it does not necessarily indicate strong coupling nor an ill-posed Cauchy problem. Through a particularly poor choice of coordinates, it is possible to make the kinetic term for superluminal fluctuations disappear even in a free theory. Likewise, information cannot propagate forward from a pathological choice of initial value surface.

On the other hand, for the  $f_o$  solution, the characteristic analysis does additionally reveal an ill-posed Cauchy problem. Since spacelike characteristics originate from the spatial origin in the open chart of de Sitter, there is no spacelike surface that intersects all characteristics. Hence this particular spacetime does *not* admit a well-defined initial value problem, as it lacks a spacelike

Cauchy surface. In contrast to superluminality, nonexistence of spacelike Cauchy surface always implies the quadratic action is pathological. Further, in contrast to the Hamiltonian identification of degrees of freedom, this concept and its relation to identifying degrees of freedom by the amount of initial data required is diffeomorphism invariant.

Finally, for the  $f_o$  solution, finite perturbations specified along characteristics diverge in amplitude at the spatial origin from which they emanate in the open chart. Given that the theory contains nonlinear interactions, this indicates that perturbation theory almost certainly breaks down leaving the theory strongly coupled there. Hence in this case, the ill-posed Cauchy problem likely originates from a point of strong coupling. More precisely, strong coupling occurs when the effective field theory breaks down due to ever higher order interaction terms becoming important. While strong coupling cannot be diagnosed from the quadratic action alone, the divergence or discontinuity of perturbative solutions at a given spacetime point is a good indicator of strong coupling there.

Vanishing of kinetic terms is often used as a related proxy for strong coupling: once variables are canonically normalized, interaction terms pick up negative powers of the coefficient in front of the kinetic term, which drives the effective strong coupling energy scale to zero when the kinetic term vanishes. However, our example shows that without examining the higher order terms themselves, one cannot immediately determine whether the vanishing of kinetic terms instead simply arises from a poor choice of coordinates.

The  $f_C$ , or stationary class of solutions, serves to further distinguish these concepts. Here generic solutions also admit spacelike characteristic curves and hence superluminality. By choosing a time coordinate that is orthogonal to these spacelike surfaces, we again recover a representation where kinetic terms and dynamics vanish in favor of spatial constraints. Unlike the open  $f_o$  solution, all characteristics of this class that are within the past light cone of an observer at the spatial origin intersect a spacelike surface. Hence the Cauchy problem is well-posed for this family of solutions and observers. Furthermore, the characteristics end rather than begin at the spatial origin where the field perturbations diverge. While strong coupling at the origin is again likely, this distinction is crucial. As in spherical collapse of perturbations in general relativity (with Newtonian gravity as the corresponding effective theory), the formation of a singularity at the origin does not necessarily invalidate the effective theory far from the singularity if nothing escapes it classically.

Finally, the new class of  $f_{ab}$  solutions serves to highlight issues with the global structure of the spacetime that can occur in theories with two metrics. In all three families of solutions, the fiducial Minkowski space does not cover the whole de Sitter spacetime. Specifically, there are points where the diffeomorphism-invariant ratio

of the determinants of the physical and fiducial metrics vanishes, diverges or is undefined. Here the spacetime becomes geodesically incomplete. While the  $f_o$  and  $f_C$  solutions allow straightforward but *ad hoc* analytic continuation past these determinant singularities to define a solution in the whole spacetime, the  $f_{ab}$  ones do not. Furthermore, since characteristics do not cross these singularities, continuity must be imposed not just for the background but also for the perturbations.

The superluminality exhibited in all three classes of solutions is a necessary condition of the bi-isotropic construction except in one unique case. Generically, starting at the bi-isotropy point characteristics are superluminal across separations comparable to the spacetime curvature as a consequence of the alignment between the locally flat spacetime metric with the fiducial flat metric. Exceptional cases produce luminal but never subluminal characteristics that intersect this worldline. For the single case of the stationary  $f_1$  solution, all characteristics are strictly luminal. Unlike the usual second-order system where characteristics define only a front velocity of discontinuous solutions, the characteristic analysis of our first-order system is fully general. In particular, it allows the construction of smooth wavepackets that also propagate superluminally and do not on their own imply strong-coupling.

While these examples do serve to distinguish the concepts of superluminality, spacelike Cauchy surfaces and strong coupling, it is important not to overinterpret their consequences for the dRGT theory itself. They represent examples of tree-level or classical propagation of perturbations on specific, perhaps pathological, self-accelerating backgrounds. Superluminality in the full theory would be in tension with the dRGT theory admitting a local and Lorentz-invariant UV completion [20]. We emphasize, however, that the characteristic analysis alone is insufficient to establish whether or not superluminal propagation is truly present—in order to discern this, it has been claimed that one must know about the Green’s function at infinite frequency [21–23], which goes beyond the classical approximation that the characteristic analysis entails.

It is also worth mentioning that the presence of superluminality does not in and of itself imply acausality [41]. Indeed, in order to establish acausality, one would need to use the superluminal propagation to construct a closed timelike curve (*e.g.*, by using a point at which characteristic curves cross). Interestingly, we find (at least in the highly symmetric case we consider) that characteristic curves only intersect at singularities, indicating that such perturbations remain causal within the effective theory, even if we equate perturbative superluminality with true superluminality. It has been conjectured in Ref. [42] that this might be true in general: the chronology protection conjecture asserts that traversing a closed timelike curve cannot be achieved within the regime of validity of the effective theory.

Finally in all of our examples, the Hamiltonian asso-

ciated with isotropic perturbations is unbounded [18]. While it is not clear how to interpret the Hamiltonian in these cases where the equations of motion are first order and there exists pathological choices of slicing where it is no longer associated with time-evolution, this may indicate that the features uncovered here are associated with an unstable background rather than generic consequences of the dRGT theory.

*Acknowledgments.*—We thank Rachel Rosen and Robert M. Wald for useful discussions. This work

was supported by the Kavli Institute for Cosmological Physics at the University of Chicago through grants NSF PHY-0114422 and NSF PHY-0551142. PM was additionally supported by grants NSF PHY-1125897 and NSF PHY-1412261 and an endowment from the Kavli Foundation and its founder Fred Kavli, WH by U.S. Dept. of Energy contract DE-FG02-13ER41958 and HM by a Japan Society for the Promotion of Science Postdoctoral Fellowships for Research Abroad. AJ was supported in part by the Robert R. McCormick Postdoctoral Fellowship.

- 
- [1] N. Arkani-Hamed, H. Georgi, and M. D. Schwartz, *Annals Phys.* **305**, 96 (2003), arXiv:hep-th/0210184 [hep-th].
- [2] P. Creminelli, A. Nicolis, M. Papucci, and E. Trincherini, *JHEP* **0509**, 003 (2005), arXiv:hep-th/0505147 [hep-th].
- [3] C. de Rham and G. Gabadadze, *Phys.Rev.* **D82**, 044020 (2010), arXiv:1007.0443 [hep-th].
- [4] C. de Rham, G. Gabadadze, and A. J. Tolley, *Phys.Rev.Lett.* **106**, 231101 (2011), arXiv:1011.1232 [hep-th].
- [5] C. de Rham, *Living Rev.Rel.* **17**, 7 (2014), arXiv:1401.4173 [hep-th].
- [6] G. D’Amico, C. de Rham, S. Dubovsky, G. Gabadadze, D. Pirtskhalava, *et al.*, *Phys.Rev.* **D84**, 124046 (2011), arXiv:1108.5231 [hep-th].
- [7] A. E. Gumrukcuoglu, C. Lin, and S. Mukohyama, *JCAP* **1111**, 030 (2011), arXiv:1109.3845 [hep-th].
- [8] P. Gratia, W. Hu, and M. Wyman, *Phys.Rev.* **D86**, 061504 (2012), arXiv:1205.4241 [hep-th].
- [9] M. S. Volkov, *Phys.Rev.* **D86**, 061502 (2012), arXiv:1205.5713 [hep-th].
- [10] M. S. Volkov, *Phys.Rev.* **D86**, 104022 (2012), arXiv:1207.3723 [hep-th].
- [11] C. de Rham, G. Gabadadze, L. Heisenberg, and D. Pirtskhalava, *Phys.Rev.* **D83**, 103516 (2011), arXiv:1010.1780 [hep-th].
- [12] K. Koyama, G. Niz, and G. Tasinato, *Phys.Rev.Lett.* **107**, 131101 (2011), arXiv:1103.4708 [hep-th].
- [13] K. Koyama, G. Niz, and G. Tasinato, *Phys.Rev.* **D84**, 064033 (2011), arXiv:1104.2143 [hep-th].
- [14] T. Nieuwenhuizen, *Phys.Rev.* **D84**, 024038 (2011), arXiv:1103.5912 [gr-qc].
- [15] L. Berezhiani, G. Chkareuli, C. de Rham, G. Gabadadze, and A. Tolley, *Phys.Rev.* **D85**, 044024 (2012), arXiv:1111.3613 [hep-th].
- [16] T. Kobayashi, M. Siino, M. Yamaguchi, and D. Yoshida, *Phys.Rev.* **D86**, 061505 (2012), arXiv:1205.4938 [hep-th].
- [17] M. Wyman, W. Hu, and P. Gratia, *Phys.Rev.* **D87**, 084046 (2013), arXiv:1211.4576 [hep-th].
- [18] N. Khosravi, G. Niz, K. Koyama, and G. Tasinato, *JCAP* **1308**, 044 (2013), arXiv:1305.4950 [hep-th].
- [19] P. Motloch and W. Hu, *Phys.Rev.* **D90**, 104027 (2014), arXiv:1409.2204 [hep-th].
- [20] A. Adams, N. Arkani-Hamed, S. Dubovsky, A. Nicolis, and R. Rattazzi, *JHEP* **0610**, 014 (2006), arXiv:hep-th/0602178 [hep-th].
- [21] S. Dubovsky, A. Nicolis, E. Trincherini, and G. Villadoro, *Phys.Rev.* **D77**, 084016 (2008), arXiv:0709.1483 [hep-th].
- [22] G. Shore, *Nucl.Phys.* **B778**, 219 (2007), arXiv:hep-th/0701185 [hep-th].
- [23] C. De Rham, L. Keltner, and A. J. Tolley, *Phys.Rev.* **D90**, 024050 (2014), arXiv:1403.3690 [hep-th].
- [24] T. J. Hollowood and J. L. Miramontes, *JHEP* **0904**, 060 (2009), arXiv:0902.2405 [hep-th].
- [25] K. Hinterbichler, A. Nicolis, and M. Porrati, *JHEP* **0909**, 089 (2009), arXiv:0905.2359 [hep-th].
- [26] M. Porrati and R. Rahman, *Phys.Rev.* **D80**, 025009 (2009), arXiv:0906.1432 [hep-th].
- [27] G. L. Goon, K. Hinterbichler, and M. Trodden, *Phys.Rev.* **D83**, 085015 (2011), arXiv:1008.4580 [hep-th].
- [28] A. Padilla, P. M. Saffin, and S.-Y. Zhou, *JHEP* **1101**, 099 (2011), arXiv:1008.3312 [hep-th].
- [29] P. de Fromont, C. de Rham, L. Heisenberg, and A. Matas, *JHEP* **1307**, 067 (2013), arXiv:1303.0274 [hep-th].
- [30] P. Cooper, S. Dubovsky, and A. Mohsen, *Phys.Rev.* **D89**, 084044 (2014), arXiv:1312.2021 [hep-th].
- [31] A. Joyce, B. Jain, J. Khoury, and M. Trodden, *Phys.Rept.* **568**, 1 (2015), arXiv:1407.0059 [astro-ph.CO].
- [32] C. de Rham, M. Fasiello, and A. J. Tolley, *Phys.Lett.* **B733**, 46 (2014), arXiv:1308.2702 [hep-th].
- [33] P. Creminelli, M. Serone, G. Trevisan, and E. Trincherini, *JHEP* **1502**, 037 (2015), arXiv:1403.3095 [hep-th].
- [34] L. Keltner and A. J. Tolley, (2015), arXiv:1502.05706 [hep-th].
- [35] S. Deser and A. Waldron, *Phys.Rev.Lett.* **110**, 111101 (2013), arXiv:1212.5835 [hep-th].
- [36] S. Deser, K. Izumi, Y. Ong, and A. Waldron, *Phys.Lett.* **B726**, 544 (2013), arXiv:1306.5457 [hep-th].
- [37] S. Deser, M. Sandora, A. Waldron, and G. Zahariade, *Phys.Rev.* **D90**, 104043 (2014), arXiv:1408.0561 [hep-th].
- [38] S. Deser, K. Izumi, Y. Ong, and A. Waldron, *Mod.Phys.Lett.* **A30**, 1540006 (2015), arXiv:1410.2289 [hep-th].
- [39] S. Deser, A. Waldron, and G. Zahariade, (2015), arXiv:1504.02919 [hep-th].
- [40] K. Izumi and Y. C. Ong, *Class.Quant.Grav.* **30**, 184008 (2013), arXiv:1304.0211 [hep-th].
- [41] E. Babichev, V. Mukhanov, and A. Vikman, *JHEP* **0802**, 101 (2008), arXiv:0708.0561 [hep-th].
- [42] C. Burrage, C. de Rham, L. Heisenberg, and A. J. Tolley,

- JCAP **1207**, 004 (2012), arXiv:1111.5549 [hep-th].
- [43] P. Gratia, W. Hu, and M. Wyman, *Class.Quant.Grav.* **30**, 184007 (2013), arXiv:1305.2916 [hep-th].
  - [44] P. Gratia, W. Hu, and M. Wyman, *Phys.Rev.* **D89**, 027502 (2014), arXiv:1309.5947 [hep-th].
  - [45] H. Motohashi and T. Suyama, *Phys.Rev.* **D86**, 081502 (2012), arXiv:1208.3019 [hep-th].
  - [46] C. Mazuet and M. S. Volkov, (2015), arXiv:1503.03042 [hep-th].
  - [47] A. E. Gumrukcuoglu, C. Lin, and S. Mukohyama, *JCAP* **1203**, 006 (2012), arXiv:1111.4107 [hep-th].
  - [48] A. De Felice, A. E. Gumrukcuoglu, and S. Mukohyama, *Phys.Rev.Lett.* **109**, 171101 (2012), arXiv:1206.2080 [hep-th].